Propagation losses in photonic crystal waveguides: Effects of band tail absorption and waveguide dispersion

Rigal, F.; Joanesarson, Kristoffer Bitsch; Lyasota, A.; Jarlov, C.; Dwir, B.; Rudra, A.; Kulkova, I.; Kapon, Eli

Published in:
Optics Express

Link to article, DOI:
10.1364/OE.25.028908

Publication date:
2017

Document Version
Publisher's PDF, also known as Version of record

Research Article | Vol. 25, No. 23 | 13 Nov 2017 | OPTICS EXPRESS 28908
Optics EXPRESS

Propagation losses in photonic crystal waveguides: effects of band tail absorption and waveguide dispersion

B. RIGAL,[1,*] K. JOANESARSON,[1,2] A. LYASOTA,[1] C. JARLOV,[1] B. DWIR,[1] A. RUDRA,[1] I. KULKOVA,[1] AND E. KAPON[1]

[1]*Laboratory of physics of nanostructures (LPN), Ecole Polytechnique Fédérale de Lausanne, CH-1015 Lausanne, Switzerland*
[2]*Department of Photonics Engineering, DTU Fotonik, Technical University of Denmark, Building 343, 2800 Kongens Lyngby, Denmark*
[*]*bruno.rigal@epfl.ch*

Abstract: Propagation losses in GaAs-based photonic crystal (PhC) waveguides are evaluated near the semiconductor band-edge by measuring the finesse of corresponding L_n cavities. This approach yields simultaneously the propagation losses and the mode reflectivity at the terminations of the cavities. We demonstrate that the propagation losses are dominated by band tail absorption for shorter wavelengths and by fabrication disorder related scattering, near the photonic band edge, for longer wavelengths. Strategies for minimizing losses in such elongated cavities and waveguides are discussed, which is important for the monolithic integration of light sources with such optical elements.

OCIS codes: (350.4238) Nanophotonics and photonic crystals, (050.5298) Photonic crystals, (230.5590) Quantum-well, -wire and -dot devices; (130.5296) Photonic crystal waveguides, (290.5880) Scattering, rough surfaces.

References and links

1. V. M. Rao and S. Hughes, "Single quantum-dot Purcell factor and β factor in a photonic crystal waveguide," Phys. Rev. B **75**, 205437 (2007).
2. D. Englund, D. Fattal, E. Waks, G. Solomon, B. Zhang, T. Nakaoka, Y. Arakawa, Y. Yamamoto, and J. Vucković, "Controlling the Spontaneous Emission Rate of Single Quantum Dots in a Two-Dimensional Photonic Crystal," Phys. Rev. Lett. **95**(1), 013904 (2005).
3. S. Hughes, L. Ramunno, J. F. Young, and J. E. Sipe, "Extrinsic optical scattering loss in photonic crystal waveguides: role of fabrication disorder and photon group velocity," Phys. Rev. Lett. **94**(3), 033903 (2005).
4. P. Dong, W. Qian, S. Liao, H. Liang, C.-C. Kung, N.-N. Feng, R. Shafiiha, J. Fong, D. Feng, A. V. Krishnamoorthy, and M. Asghari, "Low loss shallow-ridge silicon waveguides," Opt. Express **18**(14), 14474–14479 (2010).
5. L. O'Faolain, X. Yuan, D. Mcintyre, S. Thoms, H. Chong, R. M. D. L. Rue, and T. F. Krauss, "Low-loss propagation in photonic crystal waveguides," Electron. Lett. **42**, 1454–1455 (2006).
6. E. Kuramochi, M. Notomi, S. Hughes, A. Shinya, T. Watanabe, and L. Ramunno, "Disorder-induced scattering loss of line-defect waveguides in photonic crystal slabs," Phys. Rev. B **72**, 161318 (2005).
7. J. Zimmermann, H. Scherer, M. Kamp, S. Deubert, J. P. Reithmaier, A. Forchel, R. März, and S. Anand, "Photonic crystal waveguides with propagation losses in the 1dB/mm range," J. Vac. Sci. Technol. B Microelectron. Nanometer Struct. Process. Meas. Phenom. **22**, 3356–3358 (2004).
8. N. A. Wasley, I. J. Luxmoore, R. J. Coles, E. Clarke, A. M. Fox, and M. S. Skolnick, "Disorder-limited photon propagation and Anderson-localization in photonic crystal waveguides," Appl. Phys. Lett. **101**, 51116 (2012).
9. K. A. Atlasov, M. Felici, K. F. Karlsson, P. Gallo, A. Rudra, B. Dwir, and E. Kapon, "1D photonic band formation and photon localization in finite-size photonic-crystal waveguides," Opt. Express **18**(1), 117–122 (2010).
10. M. H. Baier, S. Watanabe, E. Pelucchi, and E. Kapon, "High uniformity of site-controlled pyramidal quantum dots grown on prepatterned substrates," Appl. Phys. Lett. **84**, 1943–1945 (2004).
11. A. Surrente, M. Felici, P. Gallo, B. Dwir, A. Rudra, G. Biasiol, L. Sorba, and E. Kapon, "Ordered systems of site-controlled pyramidal quantum dots incorporated in photonic crystal cavities," Nanotechnology **22**(46), 465203 (2011).
12. B. Rigal, C. Jarlov, A. Rudra, P. Gallo, A. Lyasota, B. Dwir, and E. Kapon, "Site-controlled InGaAs/GaAs pyramidal quantum dots grown by MOVPE on patterned substrates using triethylgallium," J. Cryst. Growth **414**, 187 (2014).

#304853 https://doi.org/10.1364/OE.25.028908
Journal © 2017 Received 16 Aug 2017; revised 3 Oct 2017; accepted 11 Oct 2017; published 7 Nov 2017

Optics EXPRESS

13. P. Gallo, M. Felici, B. Dwir, K. A. Atlasov, K. F. Karlsson, A. Rudra, A. Mohan, G. Biasiol, L. Sorba, and E. Kapon, "Integration of site-controlled pyramidal quantum dots and photonic crystal membrane cavities," Appl. Phys. Lett. **92**, 263101 (2008).
14. Y. Lai, S. Pirotta, G. Urbinati, D. Gerace, M. Minkov, V. Savona, A. Badolato, and M. Galli, "Genetically designed L3 photonic crystal nanocavities with measured quality factor exceeding one million," Appl. Phys. Lett. **104**, 241101 (2014).
15. R. G. Walker, "Simple and accurate loss measurement technique for semiconductor optical waveguides," Electron. Lett. **21**, 581–583 (1985).
16. A. E. Siegman, "Lasers university science books," Mill Val. CA (Edinb.) **37**, 462–466 (1986).
17. E. Kapon and R. Bhat, "Low-loss single-mode GaAs/AlGaAs optical waveguides grown by organometallic vapor phase epitaxy," Appl. Phys. Lett. **50**, 1628–1630 (1987).
18. C. Jarlov, A. Lyasota, L. Ferrier, P. Gallo, B. Dwir, A. Rudra, and E. Kapon, "Exciton dynamics in a site-controlled quantum dot coupled to a photonic crystal cavity," Appl. Phys. Lett. **107**, 191101 (2015).
19. A. F. Oskooi, D. Roundy, M. Ibanescu, P. Bermel, J. D. Joannopoulos, and S. G. Johnson, "MEEP: A flexible free-software package for electromagnetic simulations by the FDTD method," Comput. Phys. Commun. **181**, 687–702 (2010).
20. P. Lalanne, C. Sauvan, and J. P. Hugonin, "Photon confinement in photonic crystal nanocavities," Laser Photonics Rev. **2**, 514–526 (2008).
21. J. D. Dow and D. Redfield, "Toward a Unified Theory of Urbach's Rule and Exponential Absorption Edges," Phys. Rev. B **5**, 594–610 (1972).

1. Introduction

Analyzing the sources of propagation loss in semiconductor nano-photonic waveguides is important for constructing compact optical elements, with applications in integrated quantum photonics. In such applications, single photons and other non-classical states of light are generated and routed on-chip, and the selection of proper waveguiding schemes is crucial for avoiding excessive photon loss. Whereas PhC defect cavities and waveguides can provide strong optical confinement, dispersion engineering and tailored light-matter interaction that may prove crucial for on chip quantum optic devices [1,2], they may introduce high scattering losses due to the fabricated surfaces defining the PhC [3]. Alternatively, ridge waveguides have been employed to achieve lower scattering and bend losses, for longer-haul on-chip light propagation [4]. For all semiconductor waveguide types, residual, below-gap optical absorption might be particularly detrimental when light sources such as semiconductor quantum dots (QDs), made of related heterostructures, are integrated on-chip.

Strategies for minimizing propagation losses in semiconductor PhC waveguides and associated devices should consider not only inherent optical material absorption but also the impact of fabrication induced disorder and waveguide dispersion effects [3]. Experimental values of the propagation losses, extracted using different techniques, have been reported for various materials, structures and wavelengths. In Si-based PhC waveguides, propagation losses as low as 4dB/cm at 1.5μm wavelength were measured [5], and the quadratic increase in losses with increasing group index n_g due to slow light effects near the photonic bandedge was observed [6]. In GaAs PhC waveguides, propagation losses as low as 0.2 and 1.5dB/cm were reported for multimode W7 and W3 waveguides, respectively, at 1.5μm wavelength [7]. Typically, direct transmission measurements are used for extracting the propagation loss. Higher losses of 5-60dB/mm were reported for GaAs PhC W1 waveguides around 900nm wavelength by measuring the finesse of PhC cavities of different lengths [8].

In this work we analyze the wavelength dependence of the propagation losses in GaAs-based PhC waveguides by measuring the finesse of PhC L_n cavities of increasing length. The propagation losses are extracted for the wavelength range of 900-960nm, compatible with the emission wavelengths of InGaAs/GaAs QDs that can be integrated with these PhC structures. Our method yields simultaneously the mode reflectivity at the edge of the cavities, which needs to be precisely determined for accurate measurement of the propagation losses. We measured losses as low as 17dB/mm at ~910-940nm, propagation losses that are acceptable for routing single photons across distances up to ~100μm. Moreover, we show that the increased losses at shorter wavelengths due to band-tail absorption and at longer wavelengths

Optics EXPRESS

due to waveguide dispersion result in optimal wavelengths for which propagation losses are minimized.

2. Structure design and fabrication

The structures used in this study were L_n PhC membrane cavities [9] incorporating (n-1)/2 pyramidal QDs [10] with n = 3,7,17,33 and 61 [11] (9 nominally identical structures for each length). The QD-PhC structures were fabricated on a GaAs/$Al_{0.7}Ga_{0.3}As$ membrane wafer grown by molecular beam epitaxy on a (111)B GaAs substrate misoriented by 3° towards $[\bar{2}11]$. The site-controlled InGaAs/GaAs QDs were grown via metalorganic vapour phase epitaxy [12] over an array of inverted pyramids previously defined using electron beam lithography (EBL). The PhC pattern was aligned over the QDs using EBL with a ~20nm precision and etched in an inductive coupled plasma (ICP) system [13]. The 250nm thick GaAs membrane was suspended by wet etching of the sacrificial $Al_{0.7}Ga_{0.3}As$ layer. The PhC structures were designed such that their 1D photonic band overlaps the QD emission spectra [7], with a bandedge at 966nm. The hole pattern was positioned on a triangular lattice with pitch a = 225nm and 60nm radius. The QDs were distributed uniformly along the cavities at distances of 0.45µm. At each end of these cavities, three holes were shifted outwards along x by 0.23a, 0.15a and 0.048a. This cavity design improves the theoretical M_0 mode Q-factor of an L_3 cavity up to 200 000 [14]. As an example, Fig. 1 shows the design for the L_{33} cavity employed. To ensure a good spatial overlap of the QDs with cavity mode field patterns, all QDs were placed at the maxima of the in-plane electric field of the waveguide Bloch mode.

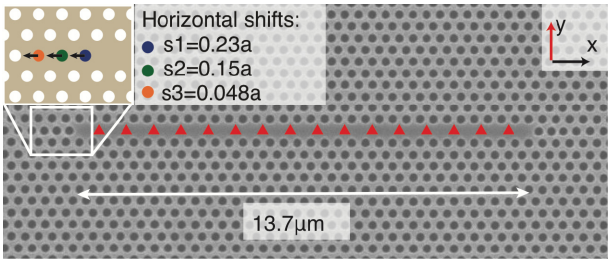

Fig. 1. Scanning electron microscope image of an L_{33} PhC cavity incorporating 16 (red triangles) embedded QDs. The inset displays the hole shifts implemented at the waveguide termination.

3. Finesse of Ln cavities

Propagation losses in optical waveguides can be extracted from measurements of the finesse of cavities formed by terminating the waveguides with reflectors to form a Fabry-Pérot (FP) resonator [15]. The finesse F of such cavities is related to the mirror reflectivity R (assumed identical at both terminations) and the distributed propagation loss coefficient α_p by [16]:

$$F = \frac{\Delta\lambda}{\delta\lambda} = \frac{\Delta\lambda}{\lambda} Q = \frac{\pi\sqrt{Re^{-L\alpha_p}}}{1 - Re^{-L\alpha_p}} \quad (1)$$

where L is the cavity length, Δλ is the free spectral range, δλ is the cavity mode spectral width, and Q is the cavity quality factor. In our case, the reflectivity is high (R≈1) the propagation losses low ($L\alpha_p << 1$), and thus the inverse of F varies approximately linearly with L:

$$\frac{1}{F} \approx \frac{1}{\pi}(1 - R + L\alpha_p) \quad (2)$$

We hence measured the finesse of the FP modes observed in the different L_n cavities versus wavelength, and used expression (1) to extract the loss and reflectivity parameters. We note

Optics EXPRESS

that when the propagation losses are comparable to the mirror losses per cavity length (i.e., when $L\alpha_p \sim \ln(1/R)$), R needs to be determined accurately enough in order to minimize the error in the extracted propagation loss [17].

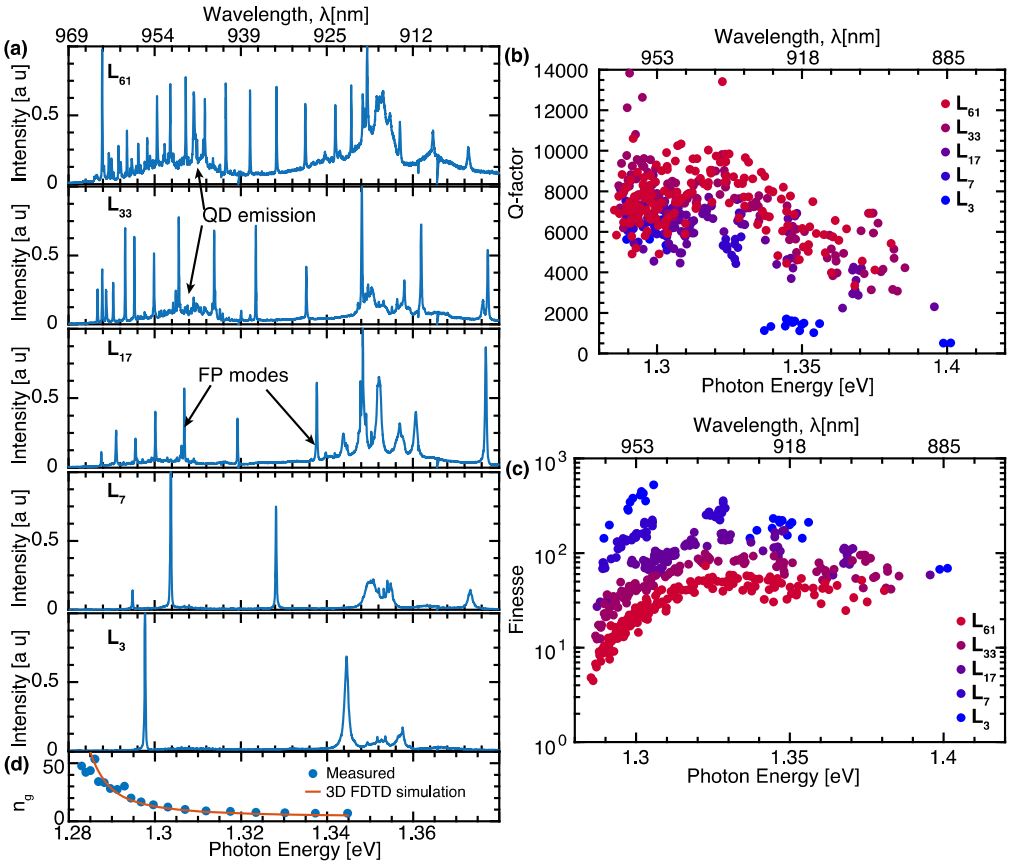

Fig. 2. (a) Photoluminescence spectra of L_n cavities of various lengths; (b) Measured Q-factors; and (c) measured finesse of the FP modes in cavities of different lengths; The inset in (b) is the power dependence of two modes in an L_{33} cavity (d) Measured and simulated group index in an L_{61} cavity (P = 500μW, T = 10K). Parameters for the 3D FDTD simulation are: n_{3D} = 3.46, slab thickness: 250nm, hole radius: 61nm. The simulated curve was shifted by 14meV to match the band edge measured from the L61 cavity.

The FP modes in the L_n cavities were identified and characterized by measuring the low temperature photoluminescence (PL) spectra of the structures. The QDs were excited with a diffraction limited 1.5μm excitation spot a relatively high power (500μW), such that a large number of FP modes were excited by emission of the dots and their barriers [18]. Spectra measured with a 70μeV resolution for representative cavities of different lengths are shown in Fig. 2(a). On the background of the broadband emission of the highly excited QDs, the FP cavity modes are clearly visible. The measured Q-factors $Q = \lambda/\delta\lambda$, where $\delta\lambda$ is the mode linewidth, were extracted with the aid of Lorentzian fits of the observed mode lineshapes, are displayed in Fig. 2(b). The measured FP mode spacing $\Delta\lambda$ in the L_{61} cavities yields the group index $n_g = \lambda^2/(2L\Delta\lambda)$ from which the finesse of the FP mode is calculated as $F = \lambda Q/(2Ln_g)$, as shown in Fig. 2(c). The measured group index of one cavity is shown on Fig. 2(d) alongside the theoretical group index computed from 3D FDTD using the software meep [19]. Group indexes up to 30 are observed. At energies below 1.286eV, the irregular values of the group indexes are a sign of Anderson localized modes which were not included in our analysis.

Optics EXPRESS

4. Analysis of propagation losses

To obtain the propagation loss coefficient as a function of wavelength, the finesse data of Fig. 2(c) were aggregated in 5nm-wide wavelength bins, and the wavelength dependence of 1/F was fitted with expression (1). Notice that the fit is very close to the linear function of L predicted by expression (2) indicating that the waveguides are in the low cavity loss regime as shown on Fig. 3(a). We restricted our analysis to the 900-960nm range, far enough from the photonic band edge in order to avoid localized modes, which cannot be described by this Fabry-Pérot model. The extracted propagation loss coefficients α_p and the transmission parameter 1-R are displayed versus wavelength in Fig. 3(b). The loss coefficient slowly decreases from 6mm^{-1} (26 dB/mm) at 910nm to 4mm^{-1} (17dB/mm) at 940nm, then increases more sharply to 17 mm^{-1} (74dB/mm) at 950-960nm, closer to the photonic band edge. This increase at longer wavelength is concomitant with the increase in the group index n_g [4], suggesting effects of slow light on the propagation losses. The reflectivity parameter R varies between 98.2 and 99.6% in the 900-950nm wavelength range; these high reflectivities are consistent with computations of reflectivity for related cavity structures [20].

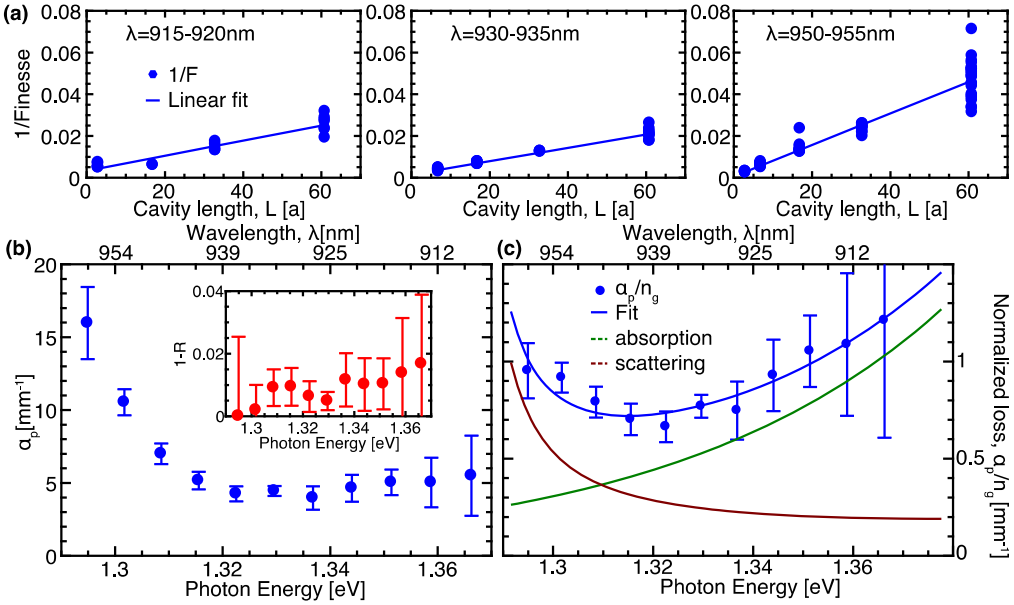

Fig. 3. (a) Measured inverse of the finesse versus cavity length (symbols) and linear fits for several wavelength ranges. (b) Extracted propagation loss coefficient α_p and reflectivity R (inset). (c) Measured (symbols) and fitted normalized loss parameter, and calculated absorption and scattering contributions (see text for definitions);

The propagation loss should increase towards the photonic band gap due to the higher group index n_g. In an attempt to uncover dispersion effects beyond a simple linear dependence on n_g, we plot in Fig. 3(c) the normalized propagation loss coefficient α_p/n_g versus wavelength. Clearly, the loss coefficient varies more rapidly than n_g at longer wavelengths. A similar increase [6] obtained via transmission measurements was attributed to backscattering and modelled as a quadratic n_g term [6]. On the shorter-wavelength side, the observed increasing loss can be explained by exponential absorption tails (e.g., Urbach tails due to lattice disorder [21]). We thus model the dependence of the propagation coefficient on photon energy E by:

$$\alpha_p = \alpha_1 e^{(E-E_{bg})/E_a} n_g + \alpha_2 n_g^2 \qquad (3)$$

Optics EXPRESS

where the first term is the absorption component and the second one represents the scattering component. Here, E_{bg} is the energy of the PhC band edge and E_a is a characteristic energy of the absorption decay. The fitted parameters (see fit in Fig. 3(c)) are: $\alpha_1 = 16 \pm 0.12\text{mm}^{-1}$, $\alpha_2 = 0.04 \pm 0.01\text{mm}^{-1}$, and $E_a = 55 \pm 21\text{meV}$. The variation of the two terms of (3), using the fit parameters, are also shown in Fig. 3(c). Two processes contributing to the propagation loss are thus distinguished in this model: absorption losses dominating at higher photon energy near the semiconductor bandedge, and scattering processes dominating at lower energy near the photonic bandedge. The propagation losses could be further decreased at longer wavelengths by shifting the photonic bandedge to lower photon energies via proper PhC designs.

Uncovering the wavelength dependence of the different loss mechanisms in these PhC waveguides also provides insight into strategies for increasing Q-factors in PhC cavities, which is important for achieving high Purcell factors and strong coupling in QD-PhC integrated structures. Estimation of the energy-decay of the band tail absorption is useful for determining the red shift of the emitter wavelength needed for reducing the absorption effects. Besides suggesting the proper red-shift in photonic band edge for minimizing the slow light effects, the scattering contribution indicates the possibility of further increase in Q-factors by selecting higher order (blue shifted) cavity modes in order to stay away from the photonic band edge.

5. Conclusion

In summary we evaluated the wavelength dependence of the propagation loss and edge reflectivity in GaAs-based PhC waveguides of finite lengths. We measured propagation losses increasing from 17 to 26dB/mm in the 900-950 wavelength range to 74dB/mm in the 950-960nm range, and waveguide edge reflectivities R~98.4-99.6% in the 908-950nm wavelength range. Moreover, we showed how the increased losses at shorter wavelengths due to band-tail absorption and at longer wavelengths due to scattering result in optimal wavelengths for which propagation losses are minimized. In particular, we demonstrated that these propagation losses are quadratic in n_g near the photonic band edge. These results are of interest for the design and optimization of integrated nanophotonic devices, e.g., semiconductor QDs embedded in PhC waveguides and cavities, in which propagation losses need to be minimized and cavity Q factors be maximized.

Funding

Swiss National Science Foundation.

Acknowledgments

This work was partly supported by the French RENATECH network. We thank Alexandre Arnoult for MBE growth of the (111)B GaAs/AlGaAs membrane wafers employed.